

We are IntechOpen, the world's leading publisher of Open Access books Built by scientists, for scientists

6,900

Open access books available

185,000

International authors and editors

200M

Downloads

Our authors are among the

154

Countries delivered to

TOP 1%

most cited scientists

12.2%

Contributors from top 500 universities



WEB OF SCIENCE™

Selection of our books indexed in the Book Citation Index
in Web of Science™ Core Collection (BKCI)

Interested in publishing with us?
Contact book.department@intechopen.com

Numbers displayed above are based on latest data collected.
For more information visit www.intechopen.com



Electrical Properties of CNT-Based Polymeric Matrix NanoComposites

Alessandro Chiolerio¹, Micaela Castellino¹, Pravin Jagdale²,
Mauro Giorcelli², Stefano Bianco³ and Alberto Tagliaferro²

¹*Physics Department, Politecnico di Torino*

²*Materials Science and Chemical Engineering Department, Politecnico di Torino*

³*Fondazione IIT (Istituto Italiano di Tecnologia), Centre for Space Human Robotics
Torino
Italy*

1. Introduction

NanoComposites (NCs) are a class of materials widely investigated in the last decade. The term NC material has broadened significantly to encompass a large variety of systems such as one-dimensional, two-dimensional, three-dimensional and amorphous materials, made of distinctly dissimilar components and mixed at the nanometer scale. The general class of organic/inorganic NC materials is a fast growing area of research. The properties of NCs depend not only on the properties of their individual elements but also on their morphology and interfacial characteristics. Large interface area between the matrix and the nano filler is a key issue for NCs.

NCs' fillers include Carbon nanomaterials. They are a large family of materials carbon based that include: fibers, nanotubes, fullerene, nano-diamonds, etc. Carbon Nanotubes (CNTs) are one of the most popular and intensively studied Carbon nanomaterials.

Since their discovery in 1991 by Iijima (Iijima, 1991), they have attracted great interest as an innovative material in most fields of science and engineering. CNTs can be thought of as sheets of graphite rolled up to make a tube. They are divided in two large classes: Multi wall CNTs (MWCNTs) and Single wall CNTs (SWCNTs). This classification depends on the number of graphite walls: several in the case of MWCNTs and only one for SWCNTs. The dimensions are variable, from few nanometers for SWCNTs to tenths of nanometers for MWCNTs. CNTs have outstanding mechanical, thermal and electrical properties.

For example as shown by Collins et al. (Collins et al., 2000) CNTs have electrical properties and electric-current-carrying capacity 1000 times higher than a copper wire. Young's module for a single-walled carbon nanotube (SWCNTs) has been estimated by Yu et al. (Yu et al., 2000) in a range of 0.32-1.47 TPa and strengths between 10 and 52 GPa with a toughness of $\sim 770 \text{ Jg}^{-1}$. A room-temperature thermal conductivity of $1750\text{--}5800 \text{ Wm}^{-1}\text{K}^{-1}$ has been estimated by Hone et al. (Hone et al., 1999).

These remarkable properties make them excellent candidates for a range of possible new classes of materials.

Several studies demonstrate how just a small percentage of CNTs loading can improve the material properties (Breuer, 2004), while still maintaining the plasticity of the polymers.

The most accessible near-term application for CNTs-polymer composite involves their electrical properties. The intrinsic high conductivity of CNTs makes them a logical choice for tuning the conductive properties of polymers. As demonstrated by MacDiarmid (MacDiarmid, 2002) CNT-added polymers are ideal candidate because they can increase the electrical conductivity by many orders of magnitude from 10^{-10} – 10^{-5} up to 10^3 – 10^5 Scm⁻¹.

CNTs production cost depends upon several parameters, one of them is the type of CNTs. In general the production of SWCNTs is more expensive than MWCNTs due to low quantity production. Purification, surface modification treatments and functionalisation also increase the cost of CNTs production. For commercialization of process it is important to use cost effective and easily reproducible CNTs i.e. MWCNTs, whose diffusion, in the last years, seems to be greater.

Depending on the specific application of CNT-based NCs, it is possible to create either an isotropic material or an anisotropic one, by orienting preferentially the CNTs: its physical properties will be in the first case independent of sample positioning and geometry, in the second case strongly geometry-dependent (Chiolerio et al., 2008). In the case of NCs prepared for electrical applications, it is desirable to create a homogeneous polymer composite.

Carboxylic functionalized CNTs (-COOH groups) for their well known easy dispersion in polymers (Gao et al., 2009) are the ideal candidate in polymer composites. In fact the modification of their surface decreases their hydrophobic nature and improves interfacial adhesion to a bulk polymer through chemical attachment. Easy and good dispersion of CNTs in the polymer matrix is essential to obtain a homogeneous final product. Small diameter CNTs, providing a uniform dispersion, means more CNTs per volume unit and as a consequence a more capillary distribution in the polymer matrix at the same weight percentage. Following these reasoning the choice of CNTs has been done on a commercial product (Nanocyl™ NC3101) ready to our purposes (see all details in experimental section). The choice of the polymers has focused on low cost materials, commercial products featuring good affinity with selected CNTs. A thermoplastic polyolefine: polyvinyl butyral (PVB) normally used in the area of glass gluing. A syloxane, Polydimethylsiloxane (PDMS) the most widely silicon-based organic polymer used. Two thermoset commercial epoxy resins: Epilox™ used in the automotive field (E) and Henkel Resin Hysol EA-9360 leader in the aerospace field (H1).

In this chapter a detailed study is presented, on the experimental conductivity and scaling laws thereof, for each of the four polymeric matrices above mentioned, as a function of the CNTs volume fraction. It will be shown that, depending on the polymer choice, it is possible to obtain NCs having a DC conductivity either showing a huge dependence on the volume fraction of CNTs or a less marked one. We also found that in one case there is no typical conductivity kink in correspondence of the percolation threshold, for the PVB matrix.

2. Experimental

2.1 Composite processing

The effective utilization of CNT materials in composite applications depends strongly on their ability to be dispersed individually and homogeneously within a matrix. To maximize the advantage of CNTs as effective reinforcement for high strength polymer composites, the CNTs should not form aggregates, and must be well dispersed to enhance the interfacial interaction with the matrix. Several processing methods are available for fabricating

CNT/polymer composites. Some of them include solution mixing, in situ polymerization, melt blending and chemical modification processes.

The general protocol for solution processing method includes the dispersion of CNTs in a liquid medium by vigorous stirring and sonication, mixing the CNTs dispersion solvents in a polymer solution and controlled evaporation of the solvent with or without vacuum conditions.

In experimental part, solution processing method was adopted for making polymer NCs. PVB and MWCNTs were treated with solvent like ethanol and butanol. Commercial thermosetting resins E, H1 and PDMS with MWCNTs followed the same method without solvent due to their liquid/viscous nature. In this way, a satisfactory level of dispersion of CNTs into the polymer matrix was obtained. Different weight % (wt.-%) concentrations of MWCNTs in polymer resin were tried to study the electrical behavior of the polymer NC.

2.2 Characterization of functionalized MWCNTs

Commercial NC3101 MWCNTs (NANOCYL™) are produced via the catalytic carbon vapour deposition (CCVD) process with average diameter 9.5 nm and average length ~ 1.5 µm (Figure 1, Field Effect Secondary Electron Microscope, FESEM).

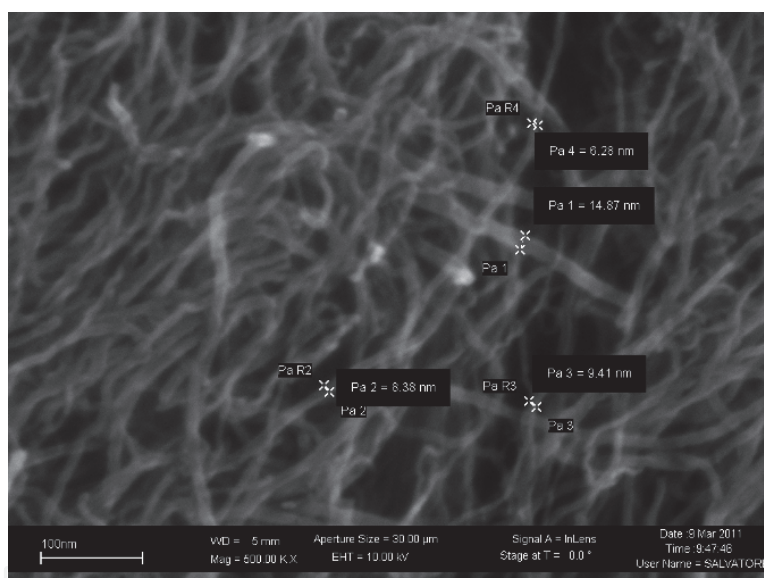


Fig. 1. FESEM image of Nanocyl™ (NC3101) Functionalized MWCNTs.

MWCNTs are then purified to greater than 95% carbon to produce the 3100 grade. This product is then functionalized with a carboxylic group (-COOH) to produce the 3101 grade. This functionalization is useful to avoid the clumps and agglomeration of MWCNTs in Polymer resin.

2.3 Thermoset epoxy resin (E)

2.3.1 Resin (T 19-36/700)

It is a commercially modified, colorless, low viscosity (650-750 mPa·s at 25 °C) epoxy resin with reduced crystallization tendency having density 1.14 gcm⁻³. Cross linking with suitable curing agents is preferably performed at room temperature. The chemical composition of Epilox resin T19-36/700 is mainly Bisphenol A (30 – 60 wt.-%), added by crystalline silica (quartz) (1 – 10 wt.-%), glycidyl ether (1 – 10 wt.-%), inert fillers (10 –60 wt.-%).

2.3.2 Hardener (H 10-31)

It is a liquid, colourless, low viscosity (400-600 mPa.s) modified cycloaliphatic polyamine epoxide adduct having density 1 gcm⁻³. Modified cycloaliphatic amine adducts.

2.3.3 Samples preparation

Resin T 19-36/700, MWCNTs and hardener H 10-31 were mixed with vigorous stirring followed by sonication. The mixture was degassed in vacuum. The mixture was poured in a mold to acquire desired shape for electrical measurements and subsequently kept in an oven at 70 °C for 4 hours for curing purposes. Electron microscopy images show the dispersion of MWCNTs in E (Figure 2).

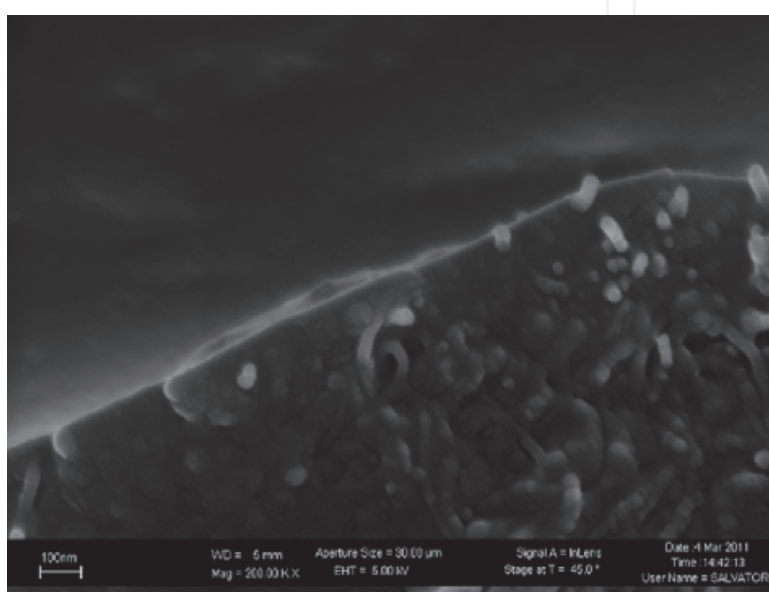


Fig. 2. FESEM of E + 5 wt.-% of MWCNTs.

2.4 Thermoset henkel resin (H1)

2.4.1 Hysol EA-9360 Part A

Henkel (Hysol EA-9360 Part A) is a white viscous paste having density 1.18 gml⁻¹. It has some interesting properties like high peel strength, excellent static stress durability, room temperature curability.

2.4.2 Hysol EA-9360 part B

Henkel (Hysol EA-9360 Part B) is a blue paste having density 1 gml⁻¹. The mixing ratio of Part A and Part B is 100:43 by weight. The chemical composition of the Henkel Part A and Part B is given below (Table 1).

2.4.3 Sample preparation

Combining Part A, Part B and MWCNTs in the correct ratio and mixing thoroughly with stirring was performed. Subsequently: degassing the mixture in vacuum, mixing of Part A and Part B which resulted in exothermic reaction (mixing smaller quantities would minimize the heat build up). The bonded parts were held in contact until the adhesive was set. Handling strength for this adhesive occurs in 24 hours (>25°C) and complete curing achieves after

Henkel Resin Hysol (EA-9360) Chemical Composition (wt.-%)			
Part A		Part B	
Epoxy resin Proprietary	30-60	Piperazine derivative Proprietary	30-60
Polyfunctional epoxy resin Proprietary	10-30	Butadiene-acrylonitrile copolymer	10-30
Synthetic rubber Proprietary	10-30	Silica amorphous (fumed)	5-10
Glass spheres Proprietary	5-10	Benzyl alcohol	5-10
Filler Proprietary	1-5	Cycloaliphatic amine Proprietary	5-10
Substituted silane Proprietary	1-5	Phenol	1-5
		Diethylene glycol Di-(3-aminopropyl)ether	1-5
		Substituted Piperazine Proprietary	1-5

Table 1. Chemical composition of Henkel Part A and Part B.

5-7 days keeping at 25 °C , for faster curing the molds were kept in the oven at 82 °C for 1 hour. Electron microscopy image shows the dispersion of MWCNTs in H1 (Figure 3).

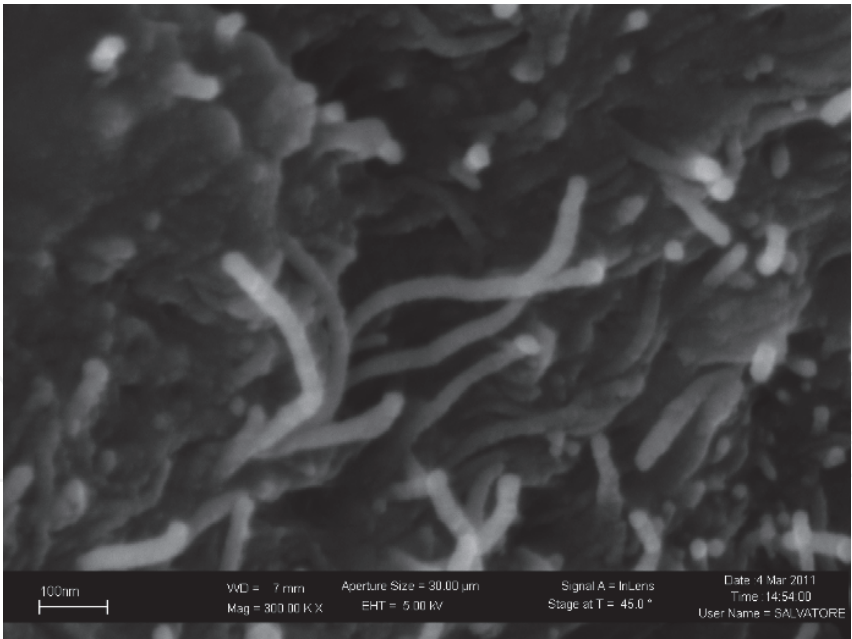


Fig. 3. FESEM of H1+ 5 wt.-% of MWCNTs.

2.5 Poly (dimethylsiloxane) (PDMS)
2.5.1 Base (Silicon Elastomer Sylgard 184 (Dow corning))

It is a Silicon based clear colourless low viscous liquid having specific gravity 1.11 gcm⁻³. It is chemically stable and not forming hazardous polymerization.

2.5.2 Curing Agent (Silicon Elastomer Sylgard 184 (Dow corning))

It is silicon resin clear colourless low viscous liquid having specific gravity 1.03 gcm^{-3} . It is also chemically stable and not forming hazardous polymerization like base. The mixing ratio of base and curing agent is 1:1 by weight and curing time for the composite is 48 hours at 25°C . Chemical formula of PDMS is $\text{CH}_3 [\text{Si} (\text{CH}_3)_2\text{O}]_n \text{Si}(\text{CH}_3)_3$. After polymerization and cross-linking, PDMS samples present an external hydrophobic surface.

2.5.3 Method for sample preparation

To ensure uniform distribution of MWCNTs, Base and Curing agent must be thoroughly mixed prior to their combination in a 1:1 ratio. The mixture was stirred and sonicated well followed by degassing in vacuum. The base and curing agent liquid mixture should have a uniform appearance. The presence of light-colored streaks or marbling indicates inadequate mixing and will result in incomplete cure. Electron microscopy image shows the dispersion of MWCNTs in PDMS resin (Figure 4).

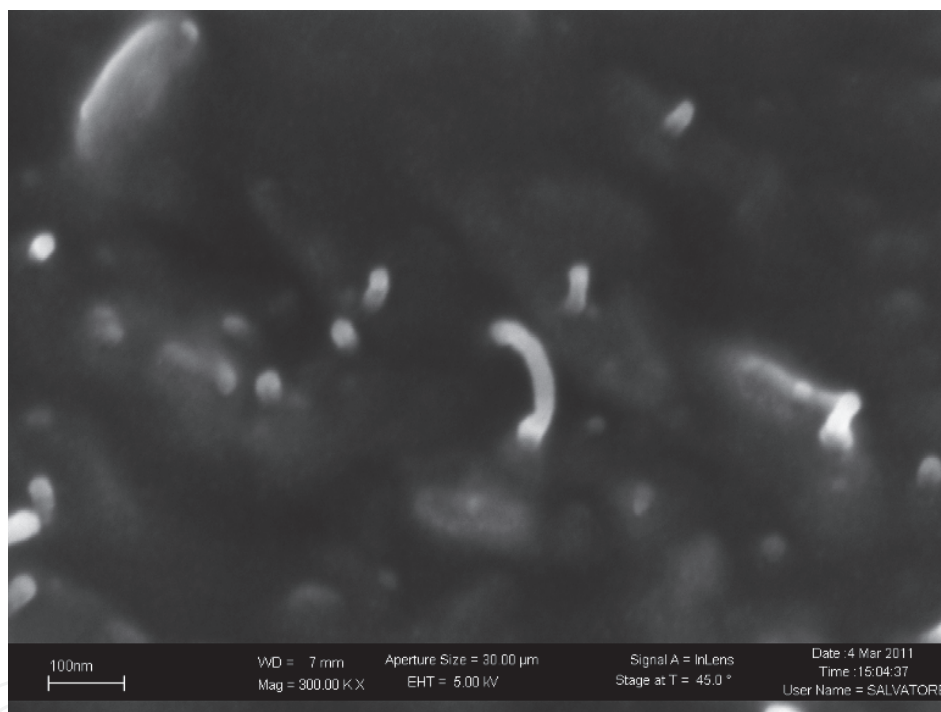


Fig. 4. FESEM of PDMS and 5 wt.-% MWCNTs.

2.6 Poly (vinyl butyral) (PVB)

PVB is a resin usually used for applications that require strong binding, optical clarity, adhesion to many surfaces, toughness and flexibility. It is prepared from polyvinyl alcohol by reaction with butyraldehyde. The IUPAC name of the polymer is Poly[(2-propyl-1,3-dioxane-4,6-diyl) methylene] with chemical structure as mentioned below (Figure 5). It is in white powder form with specific gravity 1.083 gcm^{-3} .

2.6.1 Method of preparation of PVB/MWCNTs NCs by solution processing

In preparation of CNTs-PVB (Butvar B-98, Sigma Aldrich) polymer composites, Ethanol (Carlo Erba) and 1-Butanol (Sigma-Aldrich) solvents were used with vigorous stirring and

sonication. Degassing was important for eliminating the entrapped solvent gas bubbles under vacuum. The composite was treated in oven at 70 °C for curing. Electron microscopy images show the dispersion of MWCNTs in PVB (Figure 5).

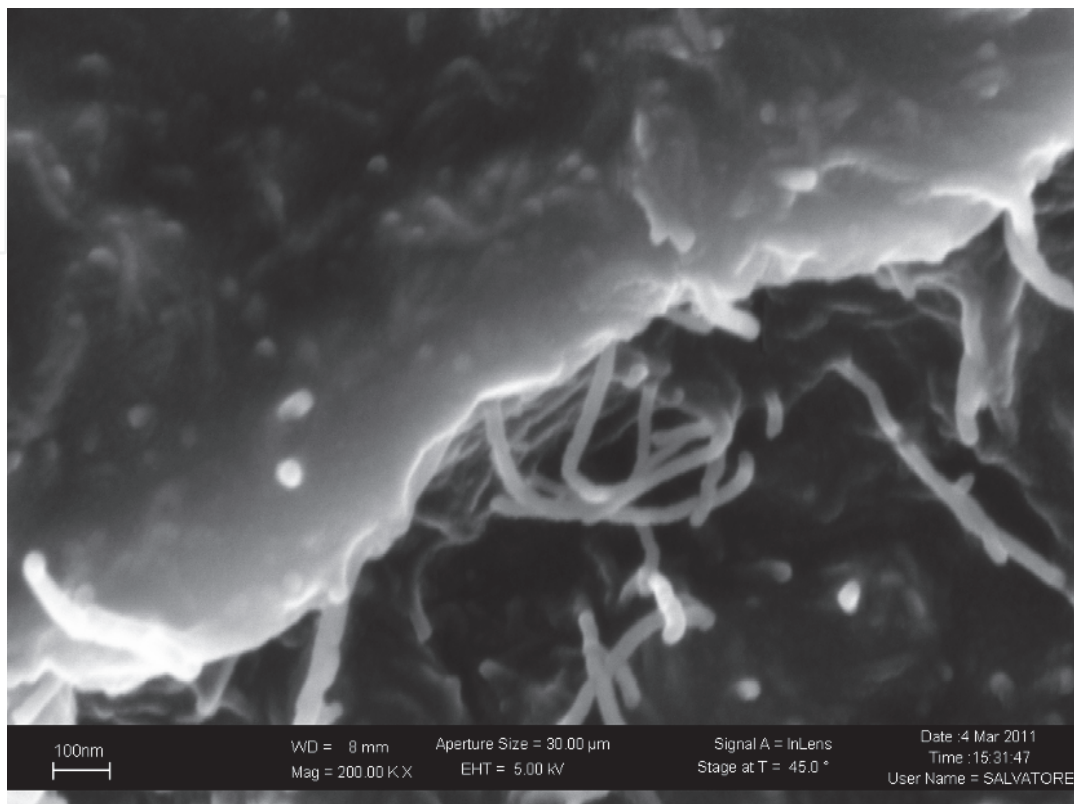


Fig. 5. PVB with 5 wt.-% of MWCNTs.

2.7 Electrical characterization

Electrical measurements were performed for each sample of the four polymer series using the so called “*Two Point Probe (TPP) method*” (Schroder, 1990)(Grove, 1993). Since we have dealt with, in principle, highly non conductive matrices, we have decided not to use the in-line “*Four Point Probes (FPP) technique*” (Smith, 1958), which is typically used for highly conductive materials, where the contact resistance between sample and connection wires could play an important role, leading to a wrong estimate of the real material resistance (Chiolerio et al., 2007).

In order to perform I-V measurements a setup already tested was chosen and used for the estimate of CNTs bundles resistivity at room temperature (Castellino et al., 2010).

In this case it was adjusted to fit our samples' dimensions. As it is possible to see from the scheme in Figure 6 a square sample was placed onto an insulating board with tin islands to place electrical connections for the Voltage supplier. To create the connections directly onto our samples surface, in an easy, fast and reproducible way, the silver conductive paste was chosen (Hu et al., 2008), which does not require any particular equipment (such as metals sputtering or thermal evaporators devices) (Coleman et al., 1998), just several minutes in order to let the solvent to evaporate. In this way it was also prevented any kind of warming of NCs or metals infiltrations during the metal contacts creation, which could have changed their properties.

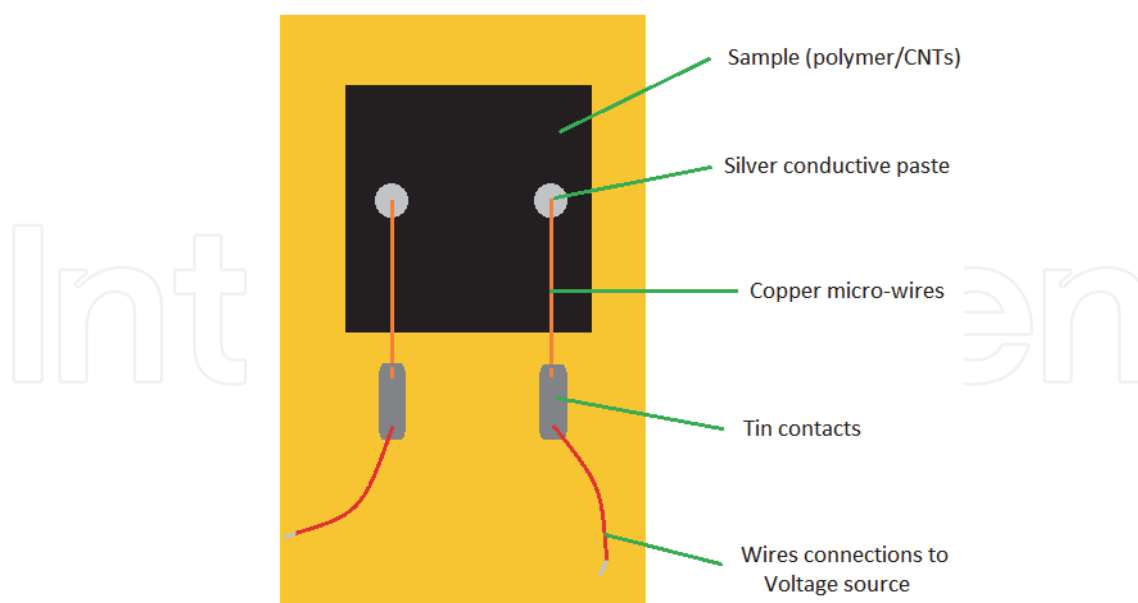


Fig. 6. Scheme of the electrical circuit device used for I-V measurements.

Insulated copper micro-wires were used to connect the Ag paste onto the sample and the tin islands on the board, since they are very thin and can be easily attached with this conductive paste. Their ends were previously exposed by means of a scalpel under an optical microscope.

A Keithley-238 High Current Source Measure Unit was used as high voltage source and nano-amperometer. It can supply up to ± 110 V and measure up to ± 1 A (at ± 15 V) and down to 10 fA.

Each sample was measured three times to have a statistical average value for the resistance and to see if the behavior observed was reproducible. For this purpose electrical connections between the voltage supplier and the board were removed every time before each measure.

For samples with 0 wt.-% CNTs the I-V measurements were performed in the range between ± 110 V with a voltage step of 1 V, in order to observe a sort of trade in the very noisy curve where the current was $I \sim 10^{-11} - 10^{-10}$ A (see Figure 7 upper panel) to obtain a sort of “zero value” for the conduction (σ_0), which will be used further in the results and discussion section for the percolation theory fit.

Instead a narrower range (± 10 V or ± 20 V, with a step of 0.1 V) was chosen for samples with wt.-% CNTs ≥ 1 mainly for two reasons:

- to avoid samples warming due to high current flow;
- since the voltage supplier possesses a threshold cut-off for currents higher than 1 A.

The first phenomenon has been observed especially with samples with a CNTs load equal or higher than 4 wt.-%. For this reason the range was moreover reduced between ± 7 or ± 3 V for some highly conductive samples (see Table 2 and Figure 7 lower panel).

In fact for E and PDMS composites a huge warming of the samples was observed, especially for PDMS + 5 wt.-% CNTs, which produced fumes from the silver paste.

On the other hand H1 NCs showed quite standard behaviors, showing an increase in the conductivity due to the increase in the CNTs amount, with no remarkable aspects to be noticed.

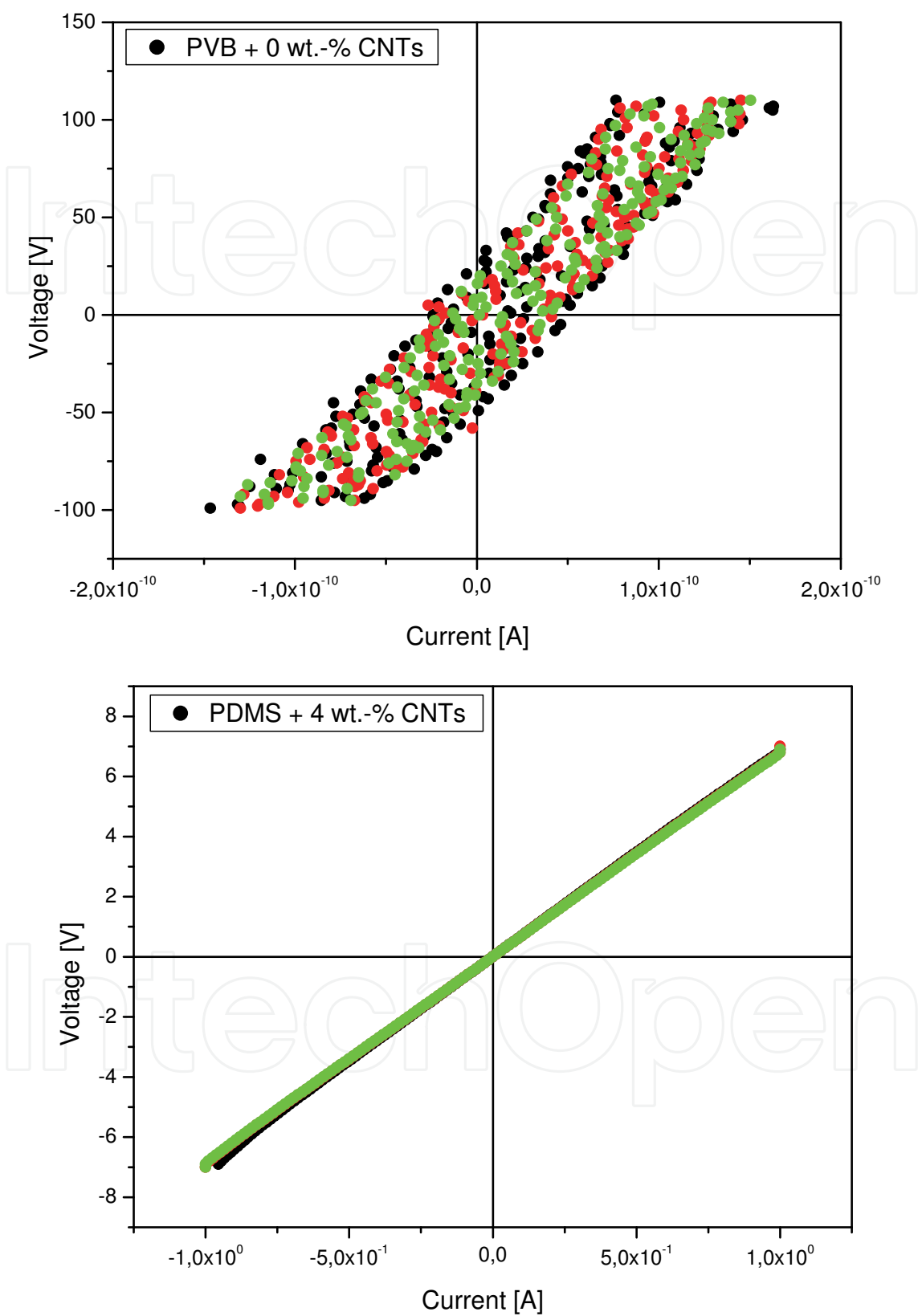


Fig. 7. Noise curves of samples PVB + 0 wt.-% CNTs (upper panel) and reduced voltage range measurements for sample PDMS + 4 wt.-% CNTs (lower panel).

Polymer	wt.-% CNTs	Voltage range (± V)	Voltage step (V)	Current range (± A)
E	0	110	1	1×10^{-10}
	1	10	0.1	2×10^{-4}
	2	10	0.1	3×10^{-2}
	3	10	0.1	3×10^{-1}
	4	10	0.1	8×10^{-1}
	5	7	0.1	8×10^{-1}
H1	0	110	1	2×10^{-10}
	1	110	1	1×10^{-10}
	2	10	0.1	1.5×10^{-6}
	3	10	0.1	3×10^{-4}
	4	10	0.1	1.5×10^{-2}
	5	10	0.1	4×10^{-2}
PDMS	0	110	1	1×10^{-10}
	1	10	0.1	1×10^{-3}
	2	10	0.1	1×10^{-1}
	3	10	0.1	5×10^{-1}
	4	7	0.1	1×10^0
	5	3	0.1	4×10^{-1}
PVB	0	110	1	1.5×10^{-10}
	1	10	0.1	2.5×10^{-10}
	2	10	0.1	8×10^{-5}
	3	20	0.1	6×10^{-5}
	4	10	0.1	2×10^{-3}
	5	10	0.1	6×10^{-3}

Table 2. Voltage (supplied) and current (registered) ranges for each sample.

3. Results and discussion

3.1 Finite element method simulation

Electrical resistivity measures were performed on the samples produced as described in the previous section. Figure 8 shows the sample geometry and the layout of the silver electrodes, placed in the 2-point configuration.

A Finite Element Method simulation was performed, using the commercial code Comsol Multiphysics™, of a composite material slab characterized by different resistivities, having the same dimensions of real samples, with the aim of evaluating the volume interested by the higher fraction of current density and estimating the penetration depth of DC currents into the sample thickness. An example of the simulation control volume is given in Figure 9, where the tetrahedral mesh of Lagrangian cubic elements is shown. The complexity of the system was quite high, having 162 k degrees of freedom and 111 k elements composing the

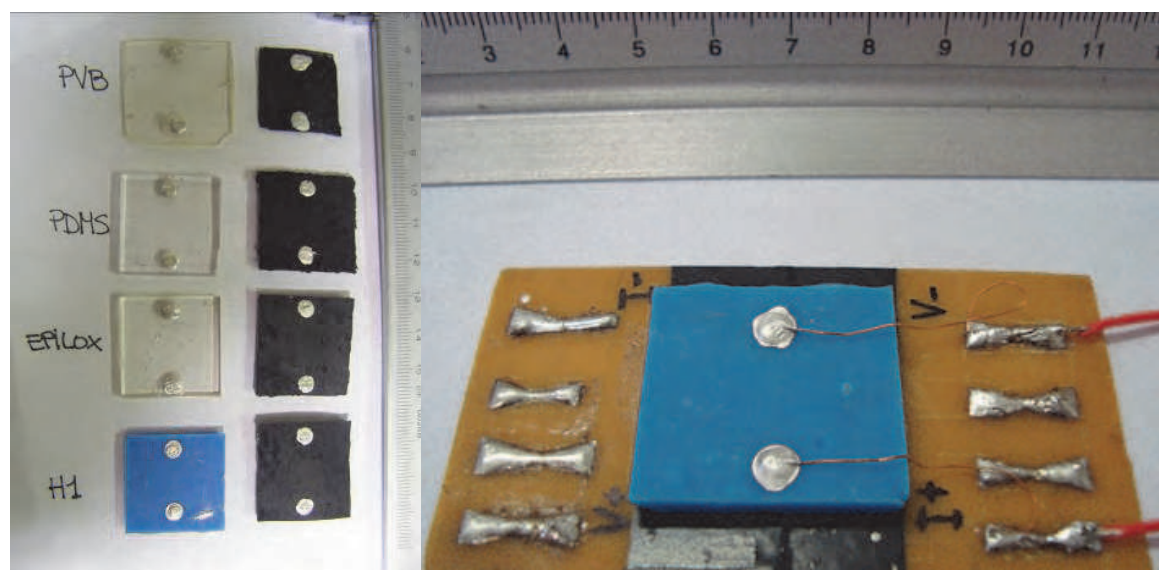


Fig. 8. Samples ready for electrical measurements; left panel: left column, pure matrices; right column, composites containing 5 wt.-% of CNTs. Right panel: sample placed in the fixture used for DC measurements.

mesh, with a solution time of more than 315 s (Intel™ Core® 2 Quad Q9550 2.83 GHz 4 GB DDR3).

As it can be seen in Figure 10, the current density is distributed almost in the whole sample, with the exception of the portions close to the electrodes, where the effective path avoids the sample bottom and edges. Based on these simulations, the effective electrical path was estimated to be: 3 mm thick (same thickness of the sample), 3 cm width (same width of the sample) and 1 cm long (sample length reduced by the electrode size and dead ends).

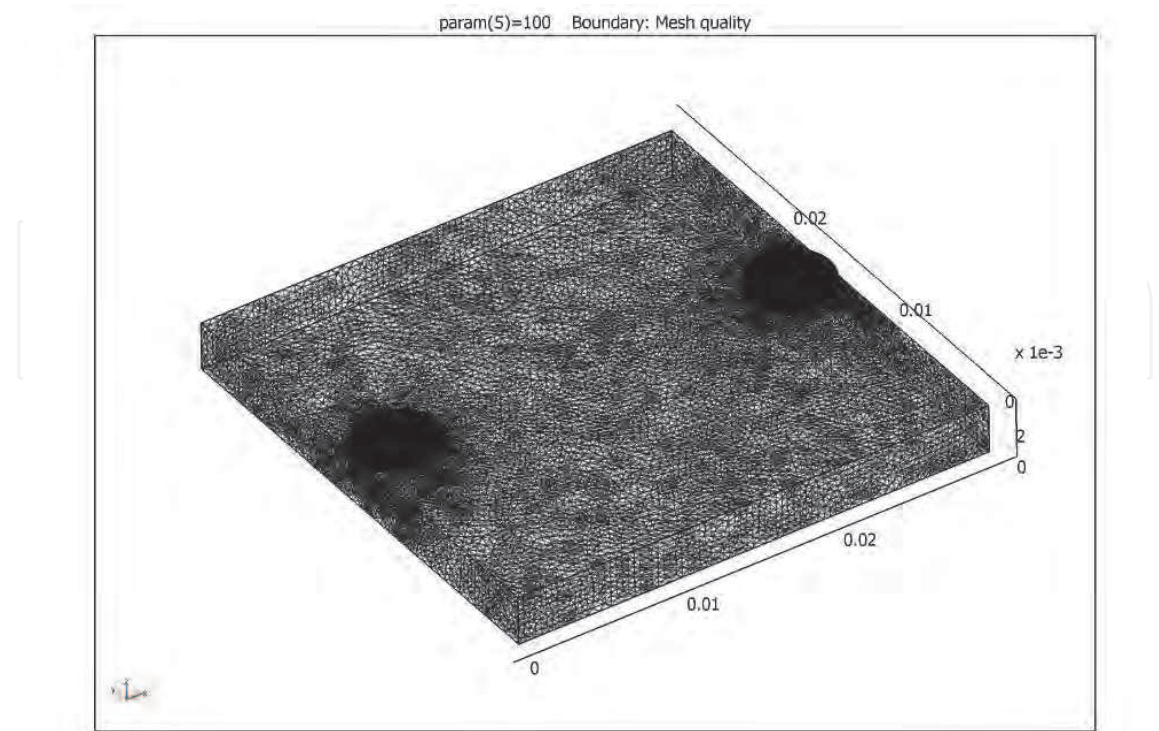


Fig. 9. Mesh distribution on the control volume of the FEM simulation.

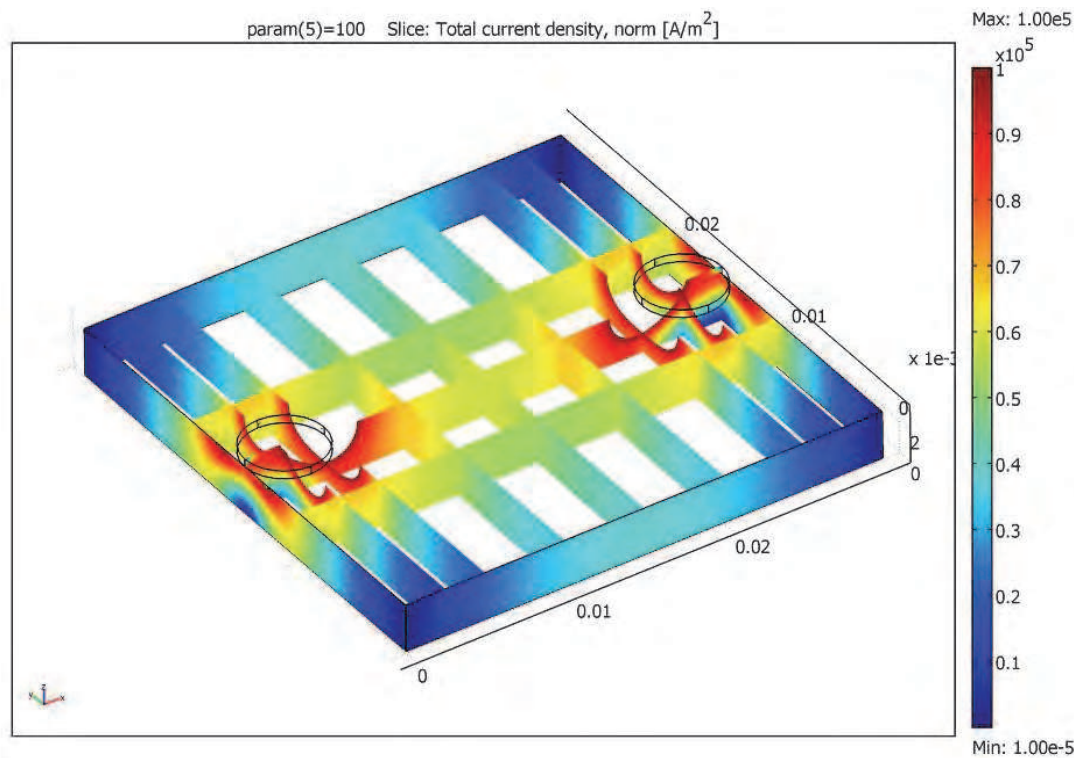


Fig. 10. Current density distribution in a composite volume.

3.2 DC conductivity and scaling laws thereof

NCs samples showed two different electrical behaviors: linear response and non-linear response, in the voltage range ± 10 V. In particular, samples characterized by the PDMS, PVB and E matrices, at low dispersoid concentrations, resulted in a symmetric nonlinear response, as shown in Figure 11. In particular, at least two regimes were observed, that typical of PDMS composites, having higher conductivities (mA range under 10 V) and that typical of PVB composites, having much lower conductivities (μ A range under 10 V). The same samples, by increasing the amount of CNTs, resulted in a perfect linear response (Figure 12), as well as H1 samples.

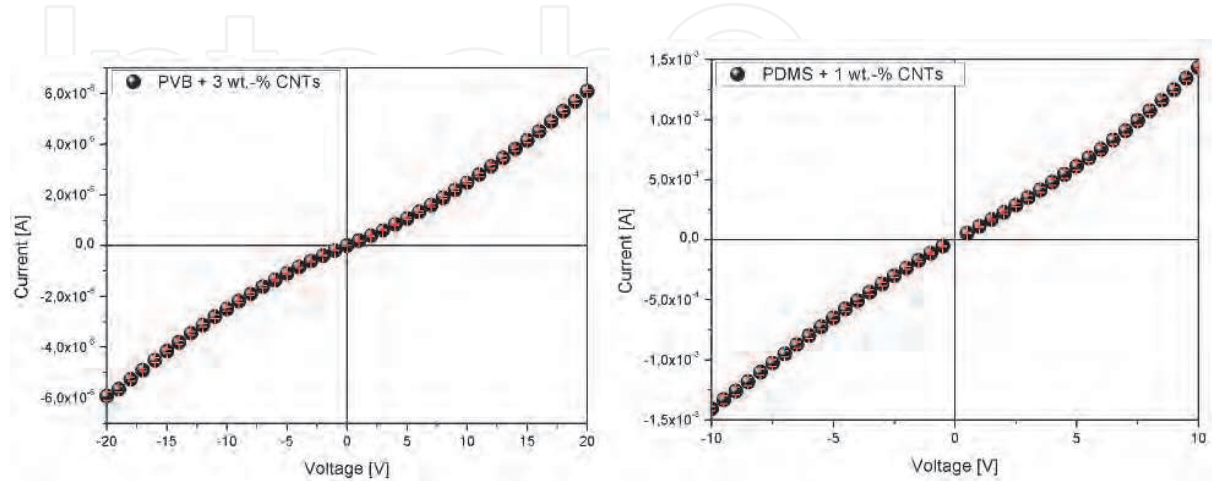


Fig. 11. Nonlinear response of samples PVB + 3 wt.-% CNTs (left panel) and PDMS + 1 wt.-% CNTs (right panel). For clarity, only 1 experimental point every 5 is shown.

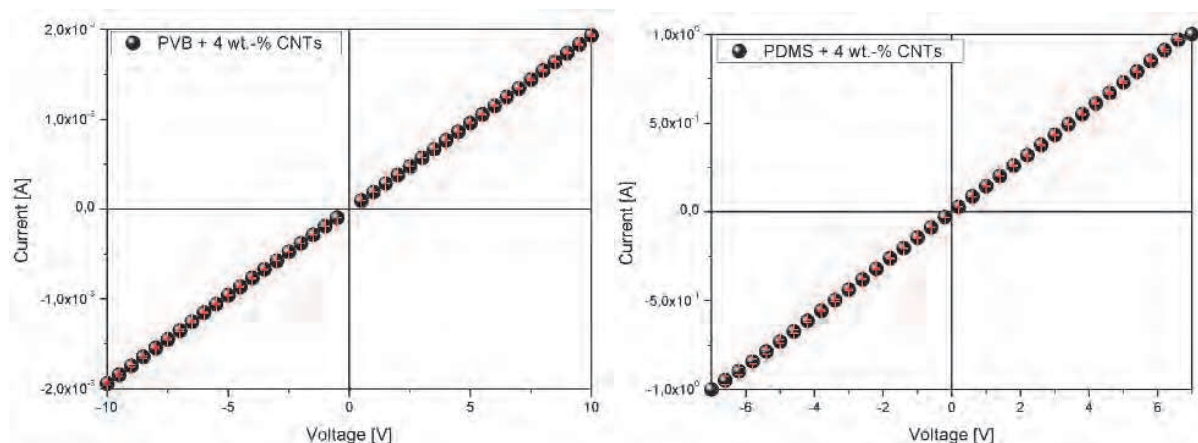


Fig. 12. Linear response of samples PVB + 4 wt.-% CNTs (left panel) and PDMS + 4 wt.-% CNTs (right panel). For clarity, only 1 experimental point every 5 is shown.

In literature, a nonlinear behavior was observed in composites based on MWCNTs networks dispersed in PDMS rubber even though the authors report no transition towards a linear response by increasing the amount of dispersoid (Liu and Fan 2007).

A possible explanation is given by the fluctuation-induced tunnelling mechanism acting in correspondence of CNTs' intersections. Some intersections, occurring between a metallic and a semiconductive CNTs, result in a Schottky barrier; when the dispersoid amount is low enough that no percolative random walks are formed going through point contact intersections, Schottky-like intersections play a major role and influence the macroscopic behavior of the NC. The energy necessary for the carriers to tunnel across the potential barrier consistent with a certain amount of polymer spacer placed between two CNTs is given by local temperature oscillations (Sheng, 1978).

In order to model the results obtained for conductivity for the different NCs as a function of the dispersoid amount, percolation theory was used as universal framework to describe physical properties of disordered systems (Stauffer & Aharony, 1994). Conductivity was computed by fitting the experimental data at high field values, thus neglecting eventual nonlinear effects which appear in the low voltage region. The idea behind the theory is that, given a lattice of a certain dimensionality and coordination, representing the dissipative or insulating matrix, a certain concentration of conductive nodes is randomly added to the system. By increasing the number of conductive nodes beyond a certain limit, said percolation threshold, a complete random walk across the lattice is made available to the carriers and a conductive behavior is observed.

$$\sigma \propto (p-p_c)^t \quad (1)$$

Equation (1) indicates that conductivity σ is proportional to a quantity depending on the volume fraction p of conductive dispersoid, on the percolation threshold p_c and on a universal scaling exponent t . Figure 13 shows the fit to experimental data, relative to our samples. The extrapolated parameters are expressed in Table 3. Generally the model seems unsuitable to fit experimental data relative to the PVB NCs: no clear transition between insulating and conductive behavior is seen and the trend of conductivity versus CNTs volume fraction is linear, in semi-logarithmic scale (Figure 13, left panel). Remarkable is the case of matrix H1, showing an insulating state even when added by more than 1 v.-% of CNTs. E and PDMS matrices, for comparison, present a clear transition. Referring to Table 3 data, we can see that the lowest percolation threshold was found for E resin (0.2 ± 0.1 v.-%),

followed by PDMS (0.7±0.2 v.-%). The critical exponent t is always close to 2.0, which is the expected value for a 3-dimensional sample (Kilbride et al., 2002).

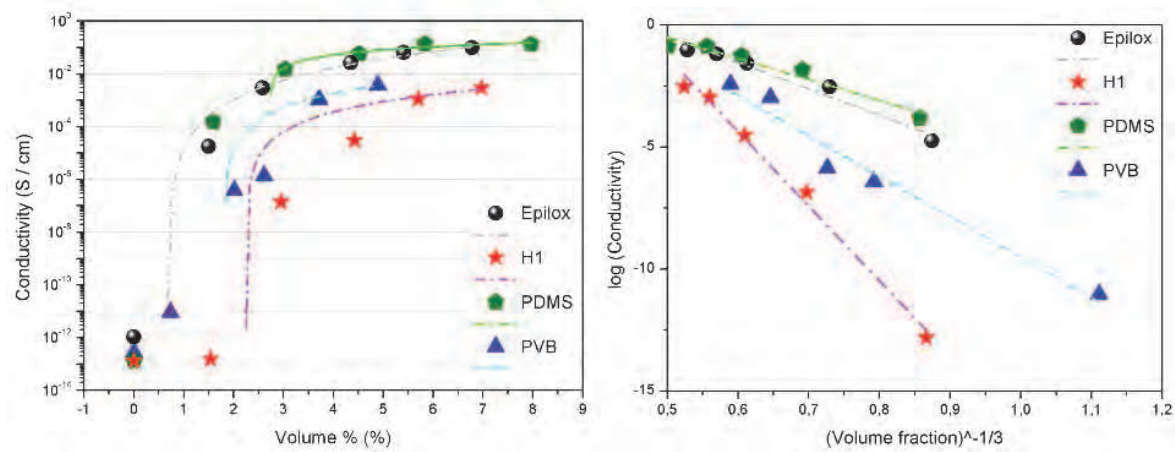


Fig. 13. Left panel: DC conductivity as a function of dispersoid volume fraction fitted by percolation model of Equation (1). Right panel: fit to experimental data according to the fluctuation-assisted tunnelling model of Equation (2).

Considering the real geometry of practical samples, physical models must be modified to take into account in particular the probability and nature of a contact between dispersoids. For example both computations and experiments show that the aspect ratio of the dispersoid plays an important role for the resulting composite properties: in particular, high aspect ratio materials (Balberg, 1987) result in a lower percolation threshold with respect to spherical particle ones (Chiolerio et al., 2010). An interesting simplification of the fluctuation-induced tunnelling for constant temperature (Kilbride et al., 2002), assuming that the CNT content is homogeneously dispersed, results in a scaling of the conductivity according to Equation 2:

$$\ln \sigma = -Ap^{-1/3} \tag{2}$$

This means that, under constant temperature, the electrical behavior is described by fluctuations depending on the mean distance between CNTs, which determines the potential barrier height. A fit to experimental data according to Equation (2) is presented in Figure 13, right panel. The model provides a very good and universal framework to predict data for every sample considered in this chapter. Parameters extrapolated from the equation are presented in Table 3. In particular, it is possible to see from the R^2 values that the fit according to this model is more accurate. It appears that PDMS has the lowest effect on affinity, the lowest the probability that the matrix affects the dispersion geometry. When the affinity, on the contrary, is not so high, CNTs may be detached from the matrix and increasing their concentration may have a smoother effect.

Matrix	p_c [v.-%]	T	R^2	A	R^2
E	0.2±0.1	2.0±0.2	0.97	11±1	0.96
H1	2.0±0.1	2±1	0.90	31±2	0.99
PDMS	0.7±0.2	2.7±0.5	0.91	9±1	0.93
PVB	2.0±0.1	2±1	0.84	17±2	0.97

Table 3. Properties of the PMNCs as extrapolated from models in Equation (1) and (2).

4. Conclusions

In conclusion we prepared four sets of NCs, using four commercial polymeric matrices (E, H1, PDMS and PVB), by dispersing an increasing amount of functionalized MWCNTs. Aim of our work was the easy preparation of cost-effective materials for electrical applications. A detailed characterization, made making use of sophisticated FEM simulations and a careful realization of a measurement setup, allowed to collect confident estimates for the resistivities and to apply physical models such as the percolation theory and the fluctuation-mediated tunneling theory. Parameters extracted from the model fitting allowed us to conclude that the lowest percolation threshold may be found for resin E; the PDMS resin shows the lowest variation of electrical properties by addition of CNTs, even though the matrix conductivity is quite high even with a very low amount of CNTs. On the contrary, resin H1 shows the higher variation of electrical resistance by addition of CNTs. Finally, PVB NCs show an interesting threshold-free behavior, consisting in a linear variation of logarithmic conductivity versus CNTs volume fraction.

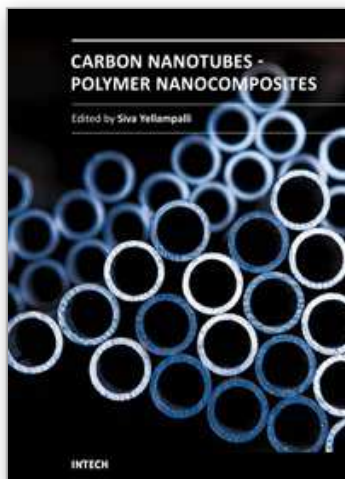
5. Acknowledgments

The Authors would like to acknowledge Dr. Salvatore Guastella and Mr. Edoardo Benassi for their precious help.

6. References

- Ajayan PM, Stephan O, Colliex C, Trauth D (1994). Aligned carbon nanotube arrays formed by cutting a polymer resin-nanotube composite, *Science* Vol. 265, (1994), pp.1212-4
- Balberg, I. (1987). Tunneling and nonuniversal conductivity in composite materials. *Physical Review Letters*, Vol.59, No.12, (1987), pp. 1305-1308
- Breuer O., Sundararaj U. (2004). Big returns from small fibers: a review of polymer/carbon nanotube composites, *Polymer Composite* Vol. 25, (2004), pp.630-645
- Castellino, M.; M. Tortello, S. Bianco, S. Musso, M. Giorcelli, M. Pavese, R. S. Gonnelli, A. Tagliaferro (2010). Thermal and Electronic Properties of Macroscopic Multi-Walled Carbon Nanotubes Blocks, *Journal of Nanoscience and Nanotechnology*, Vol. 10 (2010), p. 3828-3833, ISSN: 1533-4880
- Chiolerio, A., Allia P., Chiodoni A., Pirri F., Celegato F. and Coisson M. (2007). Thermally evaporated Cu-Co top spin valve with random exchange bias. *Journal of Applied Physics*, Vol.101, (2007), pp. 123915-1-123915-6
- Chiolerio, A., Musso S., Sangermano M., Giorcelli M., Bianco S., Coisson M., Priola A., Allia P. and Tagliaferro A. (2010). Preparation of polymer-based composite with magnetic anisotropy by oriented carbon nanotube dispersion. *Diamond and Related Materials*, Vol.17, (2008), pp. 1590-1595
- Chiolerio, A., Vescovo, L. and Sangermano, M. (2010). Conductive UV-cured acrylic inks for resistor fabrication: models for their electrical properties. *Macromolecular Chemistry and Physics*, Vol.211, (2010), pp. 2008-2016
- Coleman, J. N. ; S. Curran, A. B. Dalton, A. P. Davey, B. McCarthy, W. Blau, and R. C. Barklie (1998). Percolation-dominated conductivity in a conjugated-polymer-carbon-nanotube composite, *Physical Review B*, Vol. 58 (1998), pp. R7492-7495

- Coleman JN, Khan U, Blau WJ & Gun'ko YK. (2006). Small but strong: a review of the mechanical properties of carbon nanotube polymer composites, *Carbon* Vol. 44, (2006), pp.1624-52
- Collins P.G., P.Avouris, *Scientific American*, Vol.283, (2000), 62
- Gao Guan-hui, Chen Shou-gang, Xue Rui-ting, Yin Yan-sheng (2009), Study on the surface modification and dispersion of multi-walled carbon nanotubes, *Advanced Material Research*, Vols. 79-82, (2009), pp. 609-612
- Grove, A. S. (1993). *Physics and Technology of Semiconductor Devices*, Wiley & Sons, 1993
- Hone J, Piskoti C, Zettl A. Thermal conductivity of single-walled carbon nanotubes. *Physics Review B*, Vol.59(4), (1999), R2514-6
- Hu, N. ; Yoshifumi Karube, Cheng Yan, Zen Masuda, Hisao Fukunaga (2008). Tunneling effect in a polymer/carbon nanotube nano composite strain sensor, *Acta Materialia*, Vol. 56, (2008), pp. 2929-2936
- Iijima S., (1991). Helical microtubules of graphitic carbon, *Nature*, Vol.354, p. 56-8
- Kilbride B.E., Coleman J.N., Fournet P., Cadek M., Drury A., Hutzler S., Roth S. and Blau W.J. (2002), Experimental observation of scaling laws for alternating current and direct current conductivity in polymer-carbon nanotube composite thin films, *Journal of Applied Physics*, Vol. 92, (2002), pp. 4024-4030
- Liu, C.H. & Fan S.S. (2007). Nonlinear electrical conducting behaviour of carbon nanotube networks in silicone elastomer. *Applied Physics Letters*, Vol.90, (2007), pp. 041905-1-041905-3
- MacDiarmid, A.G. (2002). Synthetic metals: a novel role for organic polymers. *Synth. Metals*, Vol. 125, pp. 11-22, ISSN: 0379-6779
- Moniruzzaman M, Winey KI. (2006). Polymer nanocomposites containing carbon nanotubes, *Macromolecules* Vol. 39, (2006), pp.5194-205
- Schroder, D. K. (1990). *Semiconductor Material and Device Characterization*, Wiley Inter-Science Publications, 1990
- Sheng, P. (1980). Fluctuation-induced tunnelling conduction in disordered materials. *Physical Review B*, Vol.21, No.6, (1980), pp. 2180-2195
- Smits F.M. , "Measurement of sheet resistivities with the four-point probe", *Bell Syst. Tech. J.*, (1958), pp. 711-718
- Stauffer, D. & Aharony A. (1994). *Introduction to percolation theory*. Taylor and Francis, London, 1994
- Yu M.-F., B.S. Files, S. Arepalli, R.S. Ruoff, Tensile Loading of Ropes of Single Wall Carbon Nanotubes and their Mechanical Properties *Physical Review Letters*, Vol.84, (2000),5552
- <http://www.nanocyl.com/en/Products-Solutions/Products/Research-Grades/Thin-Multi-Wall-Carbon-Nanotubes>
- <http://www.leuna-harze.de/eindex.html>
- <http://www.leuna-harze.de/eindex.html>
- <http://www.dowcorning.com/applications/search/products/Details.aspx?prod=01064291&type=PROD>
- <http://www3.dowcorning.com/DataFiles/090007b2815a650e.pdf>
- <http://www3.dowcorning.com/DataFiles/090007b28147aa39.pdf>
- <http://www.sigmaaldrich.com/catalog/DisplayMSDSContent.do>



Carbon Nanotubes - Polymer Nanocomposites

Edited by Dr. Siva Yellampalli

ISBN 978-953-307-498-6

Hard cover, 396 pages

Publisher InTech

Published online 17, August, 2011

Published in print edition August, 2011

Polymer nanocomposites are a class of material with a great deal of promise for potential applications in various industries ranging from construction to aerospace. The main difference between polymeric nanocomposites and conventional composites is the filler that is being used for reinforcement. In the nanocomposites the reinforcement is on the order of nanometer that leads to a very different final macroscopic property. Due to this unique feature polymeric nanocomposites have been studied exclusively in the last decade using various nanofillers such as minerals, sheets or fibers. This book focuses on the preparation and property analysis of polymer nanocomposites with CNTs (fibers) as nano fillers. The book has been divided into three sections. The first section deals with fabrication and property analysis of new carbon nanotube structures. The second section deals with preparation and characterization of polymer composites with CNTs followed by the various applications of polymers with CNTs in the third section.

How to reference

In order to correctly reference this scholarly work, feel free to copy and paste the following:

Alessandro Chiolerio, Micaela Castellino, Pravin Jagdale, Mauro Giorcelli, Stefano Bianco and Alberto Tagliaferro (2011). Electrical Properties of CNT-Based Polymeric Matrix Nanocomposites, Carbon Nanotubes - Polymer Nanocomposites, Dr. Siva Yellampalli (Ed.), ISBN: 978-953-307-498-6, InTech, Available from: <http://www.intechopen.com/books/carbon-nanotubes-polymer-nanocomposites/electrical-properties-of-cnt-based-polymeric-matrix-nanocomposites>

INTECH
open science | open minds

InTech Europe

University Campus STeP Ri
Slavka Krautzeka 83/A
51000 Rijeka, Croatia
Phone: +385 (51) 770 447
Fax: +385 (51) 686 166
www.intechopen.com

InTech China

Unit 405, Office Block, Hotel Equatorial Shanghai
No.65, Yan An Road (West), Shanghai, 200040, China
中国上海市延安西路65号上海国际贵都大饭店办公楼405单元
Phone: +86-21-62489820
Fax: +86-21-62489821

© 2011 The Author(s). Licensee IntechOpen. This chapter is distributed under the terms of the [Creative Commons Attribution-NonCommercial-ShareAlike-3.0 License](https://creativecommons.org/licenses/by-nc-sa/3.0/), which permits use, distribution and reproduction for non-commercial purposes, provided the original is properly cited and derivative works building on this content are distributed under the same license.

IntechOpen

IntechOpen